Rate-Distortion Performance of DPCM Schemes for Autoregressive Sources

NARIMAN FARVARDIN, STUDENT MEMBER, IEEE, AND JAMES W. MODESTINO, SENIOR MEMBER, IEEE

Abstract—**An analysis of the rate-distortion performance of differential pulse code modulation (DPCM) schemes operating on discrete-time autoregressive processes is presented. The approach uses an iterative algorithm for the design of the predictive quantizer subject to an entropy constraint on the output sequence. At each stage the iterative algorithm optimizes the quantizer structure, given the probability distribution of the prediction error, while simultaneously updating the distribution of the resulting prediction error. Different orthogonal expansions specifically matched to the source are used to express the prediction error density. A complete description of the algorithm, including convergence and uniqueness properties, is given. Results are presented for rate-distortion performance of the optimum DPCM scheme for first-order Gauss–Markov and Laplace–Markov sources, including comparisons with the corresponding rate-distortion bounds. Furthermore, asymptotic formulas indicating the high-rate performance of these schemes are developed for both first-order Gaussian and Laplacian autoregressive sources.**

I. INTRODUCTION

THE EVER-GROWING DEMAND for transmission and storage of data necessitates more efficient use of existing transmission and storage facilities. A data compression system is any scheme that operates on source data to remove redundancies so that only those values essential to reproduction are retained. Typical source signals generally contain two types of redundancies: First, there is redundancy due to the high serial correlation in source outputs. This redundancy, which is concomitant with a nonuniform power spectral density, can be reduced considerably through the use of predictive encoding schemes such as differential pulse code modulation (DPCM). Roughly speaking, the source signal can be conceived as having two parts. One part is predictable relative to the transmitted sequence and hence conveys no useful information; the other part (the prediction error) is unpredictable, and since it uniquely determines the signal, it contains the useful information. A DCPM encoding scheme attempts to discard the predictable part, because it can be reproduced at the receiver, and encodes only the unpredictable portion by using a zero-memory quantizer. The second type of redundancy is due to the nonuniform probability distribution of the encoded signal. That is, the discrete levels at the output of the DPCM quantizer do not occur with equal probabilities. This type of redundancy can be removed through the optimal design of the quantizer subject to an entropy constraint, and it generally requires entropy coding of the quantizer outputs by means of a buffer-instrumented, variable-length coding scheme.

Because the quantizer is nonlinear, exact analysis of predictive coding schemes is difficult. O'Neal [1] analyzed the mean-square performance of DPCM systems for stationary Gauss–Markov processes on the assumption that the prediction error distribution is Gaussian. Others have performed an analysis of the DPCM system based on the assumption of decomposability of the prediction error into the overload and granular error [2], [3].

In contrast to these approaches, Fine [4] performed an exact analysis of the mean-square performance for a delta modulation system operating on a sampled Wiener process. Hayashi [6] extended this result to DPCM systems with an equi-step quantizer. Masry and Cambanis [11] provided an exact analysis for delta modulation of the continuous parameter Wiener process. To the authors' knowledge these are the only exact analyses concerning DPCM system performance.

Slepian [21], Arnstein [5], Hayashi [7], and Janardhanan [8], all inspired by Davisson's idea [19], [20] of obtaining a Hermite polynomial series approximation for the distribution of the prediction error, have reported various results regarding the optimality of DPCM systems in a minimum mean-square error sense for Gauss–Markov processes. Gibson and Fischer [38], on the other hand, have studied an optimal alphabet-constrained data-compression scheme that entails the DPCM system as a special case. However, little work has been done in characterizing the optimum rate-distortion performance of DPCM schemes. While there has been some limited work in approximating the optimal rate-distortion performance for Gaussian sources at high rates [9], [33], there has been no complete analysis for a wide range of rates even for Gaussian sources.

In this paper we present a study of the rate-distortion performance of DPCM schemes operating on autoregressive discrete-time sources. A novel iterative algorithm is developed for design of the DPCM quantizer to minimize the mean-square distortion subject to a constraint on the

Manuscript received October 7, 1983; revised September 13, 1984. This work was supported in part by the Office of Naval Research under Contract N00014-75-C-0281. The material in this paper was presented in part at the 1983 IEEE Symposium on Information Theory, St. Jovite, PQ, Canada.

N. Farvardin was with the Electrical, Computer, and Systems Engineering Department, Rensselaer Polytechnic Institute, Troy, NY 12180. He is now with the Electrical Engineering Department, University of Maryland, College Park, MD 20742, USA.

J. W. Modestino is with the Electrical, Computer, and Systems Engineering Department, Rensselaer Polytechnic Institute, Troy, New York 12180, USA.

0018-9448/85/0500-0402$01.00

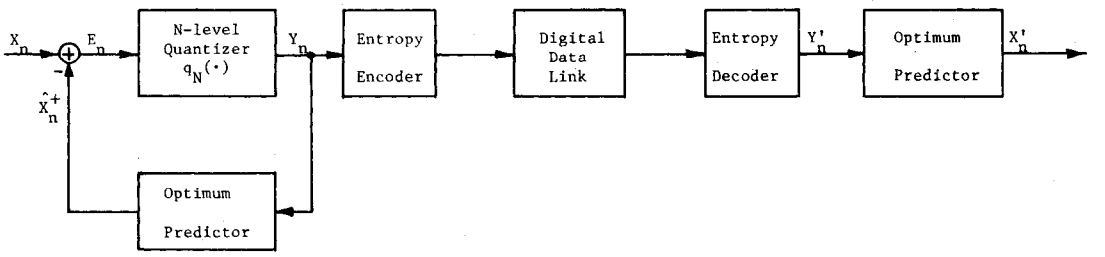

Fig. 1. Block diagram of generic predictive coding scheme.

first-order output entropy. Also, we use different orthogonal series expansions to approximate the distribution of the prediction error. These expansions are specifically matched to the distribution of the innovation sequence generating the autoregressive process. Results on the rate-distortion performance of DPCM schemes employing uniform-threshold quantizers for first-order Gauss–Markov and Laplace–Markov sources are presented. Also, asymptotic results for high rates are developed for both sources.

The organization of this work is as follows. In section II we describe a general predictive coding scheme, which is then restricted to the special case of DPCM. Then we describe certain properties of DPCM encoding schemes in Section III. In Section III we also carefully formulate the problem of optimal encoder design and determine the necessary conditions for optimality. In Section IV two algorithms for optimally designing DPCM encoders are described. Section V is devoted to a thorough study of the prediction error distribution and its evaluation through orthogonal series expansion methods. In Section VI we present numerical results demonstrating the efficacy of optimum DPCM schemes. In Section VII asymptotic results are provided for high rates, together with techniques for bounding the rate-distortion function. These latter techniques are particularly useful for characterizing the performance of non-Gaussian sources. Finally, in Section VIII a summary and suggestions for future research are included.

II. Preliminaries and Notation

In this section we briefly describe a generic predictive encoding scheme operating on an Mth-order autoregressive source. We obtain the optimum system structure for a fixed quantizer, mention the impediments in analysis and implementation of the optimum system, and then reduce the system to the suboptimum DPCM scheme for further analysis.

We assume that the signal to be encoded can be modeled as an Mth-order time-discrete autoregressive process described by the recursion

$$X_n = \sum_{m=1}^{M} \rho_m X_{n-m} + W_n, \qquad n = 1,2,\cdots, \tag{1}$$

where $\rho_1, \rho_2, \cdots, \rho_M$ are the autoregression constants and $\{W_n\}$ is a zero-mean sequence of independent and identically distributed random variables possessing common variance σ_W^2. Furthermore, we assume that the initial state $(X_0, X_{-1}, \cdots, X_{-M+1})$ is specified and we are only interested in the source outputs for $n \geq 1$.

This model has been chosen both because it is often a good mathematical model for real data (e.g., speech and images) and because it provides a well-understood standard for comparison [4]–[9], [25].

The block diagram of a generic predictive coding scheme is illustrated in Fig. 1. Upon observing the transmitted sequence $Y_1, Y_2, \cdots, Y_{n-1}$, the predictor estimates the value of the source signal at time instant n. This estimate $\hat{X}_n^+$, which can also be made at the receiver (in the absence of channel errors), is then subtracted from the input X_n to obtain the sequence $E_n = X_n - \hat{X}_n^+$, called the *prediction error*. The sequence $\{E_n\}$, which contains (almost) only "new" information about $\{X_n\}$, in then coded and transmitted as the sequence $\{Y_n\}$.

Let us assume that $\mathscr{A}_k$ is the smallest σ-algebra generated by $Y_1, Y_2, \cdots, Y_k$. Then the casual least mean-square estimate,[1] called the *predicted estimate*, of X_n upon observing $Y_1, Y_2, \cdots, Y_{n-1}$ is given by

$$\hat{X}_1^+ = 0. \tag{2a}$$

while

$$\hat{X}_n^+ = E\{X_n | \mathscr{A}_{n-1}\}, \qquad n = 2,3,\cdots, \tag{2b}$$

where $E\{\cdot|\cdot\}$ denotes conditional expectation given a σ-algebra [10].

Let us denote by $\hat{X}_n$ the *instantaneous estimate* of X_n derived by observing $Y_1, Y_2, \cdots, Y_n$ given by

$$\hat{X}_n = E\{X_n | \mathscr{A}_n\}, \qquad n = 1,2,\cdots. \tag{3}$$

Combining (1), (2), and (3) yields

$$\begin{aligned}\hat{X}_n^+ &= E\left\{\sum_{m=1}^{M} \rho_m X_{n-m} + W_n | \mathscr{A}_{n-1}\right\} \\ &= \sum_{m=1}^{M} \rho_m E\{X_{n-m} | \mathscr{A}_{n-1}\} + E\{W_n | \mathscr{A}_{n-1}\} \\ &= \rho_1 \hat{X}_{n-1} + \sum_{m=2}^{M} \rho_m E\{X_{n-m} | \mathscr{A}_{n-1}\}, \qquad n = 2,3,\cdots.\end{aligned} \tag{4}$$

The last equation is a direct consequence of the fact that $\{W_n\}$ is a zero-mean and independent sequence. Furthermore, we can write

$$\begin{aligned}\hat{X}_n &= E\{\hat{X}_n^+ + E_n | \mathscr{A}_n\} \\ &= E\{\hat{X}_n^+ | \mathscr{A}_n\} + E\{E_n | \mathscr{A}_n\}, \qquad n = 1,2\cdots.\end{aligned} \tag{5}$$

[1] Throughout this work, we confine ourselves to the squared-error distortion criterion.

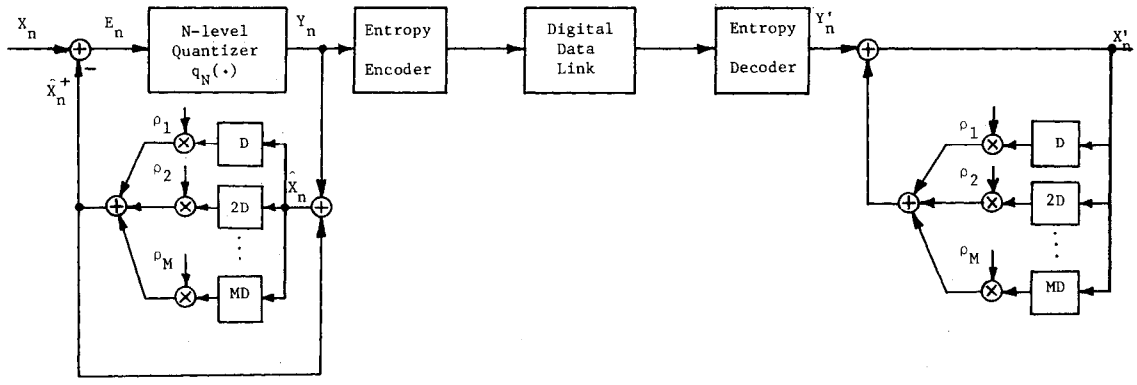

Fig. 2. Block diagram of DPCM coding system for Mth-order autoregressive source.

But $\{\mathscr{A}_n\}$ is a nondecreasing sequence of σ-algebras (i.e., $\mathscr{A}_{n-1} \subset \mathscr{A}_n$), and $\hat{X}_n^+$, by definition, is an $\mathscr{A}_{n-1}$-measurable random variable [10]. Therefore, $\hat{X}_n^+$ is $\mathscr{A}_n$-measurable as well, and (5) reduces to

$$\hat{X}_n = \hat{X}_n^+ + E\{E_n|\mathscr{A}_n\}, \qquad n = 1,2\cdots. \tag{6}$$

Unfortunately, the system described by (4) and (6) is extremely difficult—if not impossible—to implement. The conditional expectations in (4) and (6) are the main drawbacks here because they cannot be easily computed.

Our main objective is the study of the quantizer structure and its resulting effect on overall system performance. Thus, to make the problem somewhat more tractable, we force the predictor to have a simple structure.

Let us suppose that the prediction error sequence $\{E_n\}$ is "nearly" independent. This statement, although somewhat heuristic, is meaningful from a practical point of view, especially when the system is optimized (as we shall describe later) for operation at high rates. If this assumption holds, then the transmitted sequence $\{Y_n\}$ will also be nearly independent. This assumption implies that [12]

$$E\{X_{n-m}|\mathscr{A}_{n-1}\} = \hat{X}_{n-m}, \qquad n \geq m,\ 1 \leq m \leq M, \tag{7}$$

and

$$E\{E_n|\mathscr{A}_n\} = E\{E_n|Y_n\}, \qquad n = 1,2\cdots. \tag{8}$$

We assume that the prediction error is coded by means of a zero-memory N-level quantizer described by

$$q_N(x) = Q_l, \qquad x \in (T_{l-1}, T_l],\ l = 1,2,\cdots,N, \tag{9}$$

where $T_0, T_1, \cdots, T_N$, and $Q_1, Q_2, \cdots, Q_N$ are the threshold levels and the quantization levels, respectively. (To the extent possible, we use notation identical to that of [13].)

Then we can show, in Theorem 1, that

$$E\{E_n|Y_n\} = Y_n, \qquad n = 1,2,\cdots, \tag{10}$$

provided only that the quantization levels are chosen optimally.

With these simplifications, (4) and (6) can be written as

$$\hat{X}_n^+ = \sum_{m=1}^{M} \rho_m \hat{X}_{n-m}, \qquad n = 2,3,\cdots, \tag{11a}$$

and

$$\hat{X}_n = \hat{X}_n^+ + Y_n, \qquad n = 1,2\cdots. \tag{11b}$$

Equation (11) describes the simplified version of our predictive coding scheme. This scheme, which is well known as differential pulse code modulation, has been widely discussed in the literature [1]–[9]. The block diagram of this system is illustrated in Fig. 2. In the rest of this work we will restrict attention to this scheme.

Our goal is to design the quantizer in such a way that the DPCM coding scheme is optimized in a rate-distortion theoretic sense. More specifically, we wish to minimize the overall average distortion, while the transmission rate is kept below a prescribed level. In the following section, we will establish certain properties of the DPCM scheme under consideration and formulate the optimum design problem.

III. Properties of the DPCM Scheme and Problem Formulation

We begin this section by substantiating (10) through the following theorem.

Theorem 1: Let us assume that q_N is an N-level zero-memory quantizer with input thresholds $T_0 < T_1 < \cdots < T_N$ and output levels $Q_1, Q_2, \cdots, Q_N$ that are chosen such that Q_l, $l = 1,2,\cdots,N$ is the center of probability mass of the interval $(T_{l-1}, T_l]$. Then, if $\{E_n\}$ and $\{Y_n\}$ are the quantizer input and output sequences, respectively, and $E\{E_n\} = E\{Y_n\} = 0$, $n = 1,2,\cdots$, we have

$$E\{E_n|Y_n\} = Y_n, \qquad n = 1,2\cdots.$$

Proof: First note that

$$E\{E_n|Y_n = Q_l\} = E\{E_n|T_{l-1} < E_n \leq T_l\}, \qquad l = 1,2,\cdots,N. \tag{12}$$

But, by assumption,

$$Q_l = E\{E_n|T_{l-1} < E_n \leq T_l\}, \qquad l = 1,2,\cdots,N. \tag{13}$$

Therefore

$$E\{E_n|Y_n = Q_l\} = Q_l, \qquad l = 1,2,\cdots,N, \tag{14}$$

which proves the theorem.

Recall, that for the case of a zero-memory quantizer driven by a memoryless source, the amount of information delivered by the output process about the input process equals the entropy of the output process [26]. The follow-

ing theorem establishes a similar relationship in predictive quantization schemes.

Theorem 2: In the predictive coding scheme described by (11), if $\boldsymbol{X}^N \triangleq (X_1, X_2, \cdots, X_N)$ and $\boldsymbol{Y}^N \triangleq (Y_1, Y_2, \cdots, Y_N)$, then

$$\lim_{N\to\infty} \frac{1}{N} I(\boldsymbol{X}^N; \boldsymbol{Y}^N) = H_\infty(Y), \tag{15}$$

where $H_\infty(Y)$ is the entropy rate of the $\{Y_n\}$ sequence [27].

Proof: We have

$$I(\boldsymbol{X}^N; \boldsymbol{Y}^N) = H(\boldsymbol{Y}^N) - H(\boldsymbol{Y}^N|\boldsymbol{X}^N). \tag{16}$$

(Here, we are using the same notation as in [27].) But there is a one-to-one relationship between $\boldsymbol{X}^N$ and $\boldsymbol{E}^N \triangleq (E_1, E_2, \cdots, E_N)$. Furthermore, $\boldsymbol{E}^N$ uniquely specifies $\boldsymbol{Y}^N$. Therefore, given $\boldsymbol{X}^N$, there is no uncertainty concerning $\boldsymbol{Y}^N$, and thus

$$I(\boldsymbol{X}^N; \boldsymbol{Y}^N) = H(\boldsymbol{Y}^N). \tag{17}$$

Dividing through by N and passing to the limit on N yields the desired result.

In regard to the quantization error, (11b) can be used to show that

$$\xi_n \triangleq E_n - Y_n = X_n - \hat{X}_n, \tag{18}$$

where ξ_n is the error incurred solely by the quantization process.[2] This is interesting, since it implies that to minimize the overall reconstruction error, it suffices to minimize the quantization error.

At this point we can state the problem more precisely. We wish to design an N-level quantizer for the DPCM scheme such that the overall average squared-error distortion—or, equivalently, the average quantization error—is minimized, while the entropy rate at the quantizer output is held below a perscribed value, say H_0. Farvardin and Modestino [13] have studied a similar problem for a zero-memory quantizer driven by a memoryless stationary source.

In the present situation, unfortunately, the probability density function (pdf) of the quantizer input (i.e., the prediction error) is not known. The following discussion will provide some insight as to how this pdf can be calculated and will point out the associated difficulties.

Let us first note that

$$\begin{aligned} E_n &= \sum_{m=1}^{M} \rho_m X_{n-m} + W_n - \sum_{m=1}^{M} \rho_m \hat{X}_{n-m} \\ &= \sum_{m=1}^{M} \rho_m [E_{n-m} - q_N(E_{n-m})] + W_n. \end{aligned} \tag{19}$$

Equation (19) implies that the prediction error sequence $\{E_n\}$ is also a Markov process of the same order as the input process $\{X_n\}$. We shall confine ourselves, hereafter, to first-order processes. Those conversant with the theory of Markov processes will recognize that any Mth-order Markov process can be represented by a first-order M-dimensional Markov process.

Using the Chapman–Kolmogorov equation for the process defined by (19) with $M = 1$ and $\rho \triangleq \rho_1$, we obtain

$$P_{E_n}(x) = \int_{-\infty}^{\infty} P_W[x - \rho(y - q_N(y))]\, P_{E_{n-1}}(y)\, dy, \tag{20}$$

in which $P_{E_n}(\cdot)$ and $P_W(\cdot)$ designate the pdf's of E_n and W_n, respectively.

To be able to design the quantizer optimally, we require knowledge of the steady-state pdf of the sequence $\{E_n\}$, which will be denoted by $P_E(\cdot)$. A legitimate question, obviously, is whether such a steady-state pdf exists.

Gersho [14] was the first to study this issue in delta-modulation systems. Based on a theorem of Doob [15], he proved that under certain conditions on the source distribution, the joint distribution function of the $(X_n, \hat{X}_n)$ process converges to a unique stationary distribution, regardless of the initial condition $\hat{X}_1$ and the quantizer stepsize. This, in turn, implies the convergence of $\{E_n\}$ in distribution. Goldstein and Liu [16] subsequently extended Gersho's results to adaptive DPCM (ADPCM) systems in which the quantizer was taken to be an N-level uniform quantizer whose stepsize varies in time according to a well-described rule. Their results, of course, include nonadaptive DPCM systems as a special case.

More recently, Kieffer [17] has established a stronger type of convergence for predictive quantization schemes. Specifically, he has shown that under certain conditions the triple process $\{X_n, Y_n, \hat{X}_n\}$ is stochastically stable in the sense that the sequence $\{(1/N)\sum_{n=1}^{N} f(\boldsymbol{X}_n^\infty, \boldsymbol{Y}_n^\infty, \hat{\boldsymbol{X}}_n^\infty)\}$ converges almost surely for every bounded function f that is continuous in the first two variables and measurable in the third. Here $\boldsymbol{X}_n^\infty \triangleq (X_n, X_{n+1}, \cdots)$.

These convergence arguments are useful in establishing the desired result that the sequence of functions $\{P_{E_n}(\cdot)\}$ defined by (20) converges to a unique function $P_E(\cdot)$. In fact, if we write (20) in operator notation as

$$p_{E_n} = T p_{E_{n-1}}, \tag{21}$$

then Goldstein and Liu show that 1), assuming that probability functions exist, there exists a unique function $P_E(\cdot)$ such that [16, Theorems 5 and 6]

$$p_E = T p_E, \tag{22}$$

and 2) $p_{E_n}(\cdot)$ converges to $p_E(\cdot)$ [16, Theorem 9].

Equation (22) is equivalent to the following integral equation:

$$p_E(x) = \int_{-\infty}^{\infty} p_W[x - \rho(y - q_N(y))]\, p_E(y)\, dy. \tag{23}$$

Therefore, for a fixed quantizer $q_N(\cdot)$, the limiting marginal pdf of the prediction error can be obtained from the above integral equation. Equation (23) reveals the explicit dependence of the steady-state pdf $p_E(\cdot)$ on the quantizer structure $q_N(\cdot)$. On the other hand, to determine the optimum quantizer, the marginal pdf of the prediction

[2] Hereafter, for economy of notation, we do not indicate the time instants for which the equations hold with the presumption that they can be understood from the context.

error is required. This results in a complex interdependence between the pdf of the prediction error and the quantizer structure. Indeed, this is the main difficulty in obtaining the optimal quantizer.

Recall that we intend to design the quantizer subject to a constraint on its output entropy rate. To calculate the entropy rate at the quantizer output, however, we need to have the N-fold probability density function of the sequence $\{E_n\}$. Due to the myriad of difficulties associated with this, we restrict ourselves to the first-order entropy at the quantizer output. This clearly results in a suboptimum system. However, at high rates, where the prediction error, and hence the quantizer output, are highly uncorrelated, the entropy rate is approximately equal to the first-order entropy.

The problem of quantizer design can now be stated as follows. We wish to find an N-level quantizer $q_N^*(\cdot)$ that minimizes the average squared-error distortion incurred in the quantization operation while the first-order entropy at the quantizer output is held below a certain value. The average distortion and output entropy are given by

$$D = \sum_{l=1}^{N} \int_{T_{l-1}}^{T_l} (x - Q_l)^2 p_E(x)\, dx \tag{24}$$

and

$$H = -\sum_{l=1}^{N} p_l \log_2 p_l \quad \text{b/sample}, \tag{25}$$

respectively, where $p_E(\cdot)$ is the solution to the integral equation given by (23) and p_l is defined by

$$p_l = \int_{T_{l-1}}^{T_l} p_E(x)\, dx, \qquad l = 1, 2, \cdots, N. \tag{26}$$

Unfortunately, because of the particular type of dependence of $p_E(\cdot)$ on $q_N(\cdot)$, necessary conditions for the optimality of the quantizer cannot be expressed in a concise closed form. However, by looking at the problem from a slightly different perspective, we can obtain a more appealing formulation of the problem, which leads to an algorithmic approach for quantizer design.

More precisely, we seek and optimum N-level quantizer $q_N^*(\cdot)$ and a probability density function $p_E^*(\cdot)$ or, equivalently, a couple (q_N^*, p_E^*) such that the following two conditions are simultaneously satisfied.

Condition 1: $q_N^*(\cdot)$ is an optimum N-level quantizer with entropy constraint H_0 for a memoryless source with stationary marginal pdf $p_E^*(\cdot)$.

Condition 2: $p_E^*(\cdot)$ is the solution to integral equation (23), with $q_N = q_N^*$.

Let us denote by $D(q_N; p_E)$ the average distortion incurred in a DPCM coding scheme possessing an N-level quantizer $q_N(\cdot)$ and a steady-state prediction error pdf $p_E(\cdot)$. Then the optimum (rate-distortion theoretic) performance attainable by an N-level DPCM coding scheme is given by

$$D_N(H_0) = \inf_{\mathscr{C}} D(q_N; p_E), \tag{27}$$

where $\mathscr{C}$ is the collection of all couples $(q_N; p_E)$ satisfying Conditions 1 and 2 simultaneously.

In the following section, we describe two algorithmic methods for obtaining $D_N(H_0)$. Essentially, these algorithms work by iteratively applying Conditions 1 and 2. In Condition 1 we have to design an optimum entropy-constrained quantizer for a memoryless source. We do not elaborate on this; details, including specific algorithms, can be found in [13]. In Condition 2 we need to solve the integral equation (23). Section V is devoted to this issue.

IV. Algorithms

Recall that in obtaining the optimum quantizer, the quantities of interest are the average distortion and the quantizer output entropy, both of which are functionals of the prediction error pdf $p_E(\cdot)$ and the quantization mapping $q_N(\cdot)$, with a specific interdependence between $p_E(\cdot)$ and $q_N(\cdot)$.

The algorithm used to solve for the optimum quantizer is an iterative method in which the quantizer is optimized at each iteration and then the pdf of the prediction error is updated. This algorithm is described in the following steps.

Algorithm 1

1) Choose an initial N-level quantizer $q_N^{(1)}(\cdot)$ with entropy constraint H_0 and set $i = 0$.
2) Set $i = i + 1$; for the fixed quantizer $q_N^{(i)}(\cdot)$ solve (23) to find the steady-state pdf $p_E^{(i)}(\cdot)$.
3) For the fixed pdf $p_E^{(i)}(\cdot)$ use the quantizer design algorithm to obtain a quantizer $q_N^{(i+1)}(\cdot)$ subject to entropy constraint H_0.
4) If the difference in the quantizer structure[3] in two consecutive iterations is greater than some prescribed small $\epsilon > 0$, go to 2). Otherwise, halt with $p_E(\cdot)$ and $q_N(\cdot)$ equal to $p_E^*(\cdot)$ and $q_N^*(\cdot)$, respectively.

In step 3), either of the algorithmic methods described in [13] can be used to obtain the optimum quantizer.

Let us note that in solving (23) at each step of Algorithm 1, we calculate the steady-state pdf of the prediction error. Another approach, which is a slight modification of Algorithm 1, develops a sequence of quantizers evolving in time ultimately converging to the optimum quantizer. This approach is presented in the following.

Algorithm 2

1) Choose an initial N-level quantizer $q_N^{(1)}(\cdot)$ with entropy constraint H_0; set $p_E^{(0)}(\cdot) = p_W(\cdot)$ and $i = 0$.
2) Set $i = i + 1$; for the fixed quantizer $q_N^{(i)}(\cdot)$ use

[3] By the difference in the quantizer structure in two consecutive iterations we mean

$$\sum_{l=1}^{N-1} |T_l^{(i)} - T_l^{(i-1)}| + \sum_{l=1}^{N} |Q_l^{(i)} - Q_l^{(i-1)}|, \text{ where } T_l^{(i)} \text{ and } Q_l^{(i)},$$

are the lth threshold and quantization levels, respectively, at the ith iteration.

$p_E^{(i)} = Tp_E^{(i-1)}$ to find $p_E^{(i)}(\cdot)$. Here T is the operator defined in (21).[4]

3) For the fixed pdf $p_E^{(i)}(\cdot)$, use the quantizer design algorithm to obtain a quantizer $q_N^{(i+1)}(\cdot)$ subject to entropy constraint H_0.
4) If the difference in the quantizer structure in two consecutive iterations is greater than some prescribed small $\epsilon > 0$, go to 2). Otherwise, halt with $p_E(\cdot)$ and $q_N(\cdot)$ equal to $p_E^*(\cdot)$ and $q_N^*(\cdot)$, respectively.

The main drawback in implementing these algorithms is the inherent difficulty in calculating the pdf of the prediction error—that is, step 2) of either algorithm. In the following section, we describe a method for calculating the pdf of the prediction error and point out the associated difficulties.

V. Distribution of the Prediction Error

We now proceed to calculate the marginal pdf of the prediction error assuming that the quantizer is fixed. Equation (19), with $M = 1$ and $\rho_1 = \rho$, can be written as

$$E_n = W_n + \rho\xi_{n-1}, \tag{28}$$

where ξ_n is independent of W_m, $m > n$. Denoting the characteristic function (chf) of a random variable X by $\Phi_X(\cdot)$, we can write

$$\Phi_{E_n}(z) = \Phi_W(z) \cdot \Phi_{\xi_{n-1}}(\rho z), \tag{29}$$

and for the steady-state situation

$$\Phi_E(z) = \Phi_W(z)\Phi_\xi(\rho z). \tag{30}$$

The chf $\Phi_\xi(z)$ of the quantization error is given by

$$\Phi_\xi(z) = \sum_{l=1}^{N} e^{-jzQ_l} \int_{-\infty}^{\infty} e^{jzx} p_E(x) I_l(x)\, dx, \tag{31}$$

where $I_l(\cdot)$ is the indicator function of the interval $(T_{l-1}, T_l]$. Upon defining the Fourier transform of $I_l(\cdot)$ by

$$\psi_l(z) \triangleq \int_{-\infty}^{\infty} e^{jzx} I_l(x)\, dx, \qquad l = 1,2,\cdots,N, \tag{32}$$

and using (31), we can write (30) as

$$\Phi_E(z) = \Phi_W(z)\left[\sum_{l=1}^{N} e^{-jz\rho Q_l}\left(\Phi_E * \psi_l(\rho z)\right)\right], \tag{33}$$

in which * designates the convolution operation.

Equation (33) is the generic form of the functional equation describing $\Phi_E(\cdot)$. The integral equation (23), or its frequency domain equivalent (33), are both extremely difficult to solve, except in special cases. For $N = 2$ with $Q_2 = -Q_1 = \alpha$ and $T_1 = 0$ (i.e., delta modulation), (33) is equivalent to

$$\hat{\Phi}_E(z) = \Phi_W(z)\left[2\pi\Phi_E(\rho z)\cos\alpha\rho z + 2\hat{\Phi}_E(\rho z)\sin\alpha\rho z\right], \tag{34a}$$

where $\hat{\Phi}_E(\cdot)$ denotes the Hilbert transform [18] of $\Phi_E(\cdot)$ and is described by[5]

$$\hat{\Phi}_E(z) = \mathrm{PV}\int_{-\infty}^{\infty} \frac{\Phi_E(\lambda)}{z-\lambda}\, d\lambda. \tag{34b}$$

For the special case of $\rho = 1$ and $N = 2$, Fine [4] has solved (33) for $\Phi_E(\cdot)$ using Wiener–Hopf factorization techniques. Later, Hayashi [6] proved a very useful theorem that relates the pdf of the prediction error in a DPCM scheme with an N-level, symmetric, and uniform quantizer to that of a two-level scheme. Therefore, if attention is restricted to uniform quantization, it suffices to find the solution for a two-level quantizer.

Unfortunately, for $\rho \neq 1$, which is most interesting in many practical situations, techniques for explicit evaluation of the prediction-error distribution have not yet been developed. Therefore, one must resort to efficient numerical methods to compute this quantity. The idea of using orthogonal series expansions for computing the prediction error distribution was apparently first suggested by Davisson [19],[20]. His suggestion was then followed up by Slepian [21], Arnstein [5], Hayashi [7], and Janardhanan [8]. Each of these works considered a Gaussian input and a Hermite polynomial expansion for the pdf of the prediction error. Arnstein's work [5] is most relevant to the present study. Arnstein, however, does not attempt to optimize the system in a rate-distortion theoretic sense. Instead, he devises an algorithm (similar to Algorithm 2 of this paper) by which the quantizer is designed only to minimize the average squared-error distortion for a fixed number of quantization levels.

In what follows we consider Gauss–Markov and Laplace–Markov sources. For each source we use a "suitable" orthogonal expansion that is matched to the distribution of the innovation sequence generating the source and that therefore approximates the prediction error density with a small number of coefficients in the expansion.

A. Gauss–Markov Process

The Gauss–Markov process is defined according to (1) with $M = 1$ and $\rho_1 = \rho$, while we take $\{W_n\}$ to be a zero-mean sequence of Gaussian random variables with variance $\sigma_W^2 = 1$. It turns out that, under appropriate initial conditions, $\{X_n\}$ is a stationary zero-mean Gaussian random process with variance $\sigma_x^2 = 1/(1-\rho^2)$.

Now consider the Gram–Charlier series expressing the prediction error pdf $p_{E_n}(x)$ in terms of Hermite polynomials [22] by

$$p_{E_n}(x) = g(x)\sum_{k=0}^{\infty} \alpha_k^{(n)} H_k(x), \qquad -\infty < x < \infty, \tag{35a}$$

[4] In Algorithm 2, the iteration index i plays an identical role as the time index n in (21).

[5] The Cauchy principal value of an integral is defined by

$$\mathrm{PV}\int_{-\infty}^{\infty} f(x)\, dx = \lim_{R\to\infty}\int_{-R}^{R} f(x)\, dx.$$

where $g(x)$ is the standard normal pdf given by

$$g(x) = \frac{1}{\sqrt{2\pi}} e^{-x^2/2}, \qquad -\infty < x < \infty, \tag{35b}$$

$H_k(x)$ is defined by

$$H_k(x) = \frac{(-1)^k}{g(x)} \frac{d^k g(x)}{dx^k}, \qquad k = 0, 1, \cdots, \tag{35c}$$

and (where we assume $d^0 g(x)/dx^0 = g(x)$)

$$\alpha_k^{(n)} = \frac{1}{k!} \int_{-\infty}^{\infty} p_{E_n}(x) H_k(x)\, dx, \qquad k = 0, 2, \cdots. \tag{35d}$$

It is well known that the sequence $\{H_k(x)\}$ is orthogonal over the interval $(-\infty, \infty)$ with respect to the weighting function $g(x)$. That is,

$$\int_{-\infty}^{\infty} g(x) H_k(x) H_l(x)\, dx = k! \delta_{kl}, \qquad k, l = 0, 1, \cdots, \tag{36}$$

where δ_{kl} is the Kronecker delta function.

In (35a) the unknowns are the coefficients $\alpha_k^{(n)}$, $k = 0, 1, \cdots$. In what follows we obtain a recursive formula describing the expansion coefficients at time instant n in terms of those at time instant $n - 1$.

Let us replace $p_{E_{n-1}}(y)$ in (20) by its series expansion. Then

$$p_{E_n}(x) = \sum_{k=0}^{\infty} \alpha_k^{(n-1)} \int_{-\infty}^{\infty} p_W[x - \rho(y - q_N(y))] \cdot g(y) H_k(y)\, dy, \tag{37}$$

and therefore, the expansion coefficients at the nth time instant are given by

$$\alpha_l^{(n)} = \sum_{k=0}^{\infty} A_{l,k} \alpha_k^{(n-1)}, \qquad l = 0, 1, \cdots, \tag{38a}$$

where

$$A_{l,k} = \frac{1}{l!} \int_{-\infty}^{\infty} \int_{-\infty}^{\infty} p_W[x - \rho(y - q_N(y))] \cdot g(y) H_l(x) H_k(y)\, dx dy, \qquad l, k = 0, 1, \cdots. \tag{38b}$$

Note that $A_{l,k}$ is independent of time, and hence once $A_{l,k}$, $l, k = 0, 1, \cdots$ are calculated, we can evaluate the $\alpha_l^{(n)}$ recursively according to (38a) for all time instants.

In Appendix A we give a simplification of the double integral in (38b). Equation (38a) is, in effect, an infinite matrix multiplication. For numerical computations, however, it is necessary to consider a truncated version of (38a). We shall elaborate on this in the next section.

B. Laplace–Markov Process

The stationary Laplace–Markov process is described in [36]. By this we mean a first-order Markov process with a Laplacian marginal distribution, which is a special case of (1) with $M = 1$ and $\rho_1 = \rho$. First we determine the density of the process $\{W_n\}$ generating the Laplace–Markov process.

Upon taking chf's in (1), we have

$$\Phi_X(z) = \Phi_X(\rho z) \Phi_W(z), \tag{39}$$

in which $\Phi_X(\cdot)$ and $\Phi_W(\cdot)$ denote the characteristic functions of X_n (in steady state) and W_n, respectively. But if

$$p_X(x) = \frac{1}{2} e^{-|x|}, \qquad -\infty < x < \infty, \tag{40a}$$

as assumed, we have

$$\Phi_X(z) = \frac{1}{1 + z^2}, \qquad -\infty < z < \infty. \tag{40b}$$

Note that $\Phi_X(z) \neq 0$, and hence solving for $\Phi_W(z)$,

$$\Phi_W(z) = \frac{1 + \rho^2 z^2}{1 + z^2} = \rho^2 + (1 - \rho^2) \frac{1}{1 + z^2}, \tag{41a}$$

and thus

$$p_W(x) = (1 - \rho^2) \frac{1}{2} e^{-|x|} + \rho^2 \delta(x), \qquad -\infty < x < \infty. \tag{41b}$$

That is, $\{W_n\}$ represents a source generating a random variable whose value is either zero with probability ρ^2 or Laplacian distributed with probability $(1 - \rho^2)$. Here, again under appropriate initial conditions, the process $\{X_n\}$ is a stationary zero-mean Laplacian process with variance $\sigma_x^2 = 2$.

The significance of studying Laplace–Markov sources is the observation, made by several researchers (e.g., [23]), that speech signals possess a marginal density reasonably close to a Laplacian density.

In this case we can use Laguerre polynomials [24], for a series expansion of the prediction error pdf. The reason for this choice, which will become clear in the next section, is that Laguerre polynomials are orthogonal with respect to an exponential function $(0, \infty)$. More specifically, we can write

$$p_{E_n}(x) = l(x) \sum_{k=0}^{\infty} \beta_k^{(n)} L_k(x), \qquad 0 < x < \infty, \tag{42a}$$

where

$$l(x) = e^{-x}, \qquad 0 < x < \infty. \tag{42b}$$

Here, the kth order Laguerre polynomial $L_k(x)$ is defined for $x \geq 0$ by

$$L_k(x) = \frac{1}{k! l(x)} \frac{d^k}{dx^k}(x^k l(x)), \qquad k = 0, 1, \cdots, \tag{42c}$$

$$\beta_k^{(n)} = \int_0^{\infty} p_{E_n}(x) L_k(x)\, dx, \qquad k = 0, 1, \cdots. \tag{42d}$$

The orthogonality properties of Laguerre polynomials relative to an exponential function on $(0, \infty)$ imply

$$\int_0^{\infty} e^{-x} L_k(x) L_l(x)\, dx = \delta_{kl}. \tag{43}$$

In what follows, we assume that the quantizer possesses old symmetry. With this assumption, it is easy to show that $p_{E_n}(x)$, $n = 1, 2, \cdots$, has even symmetry, and hence the integral in (20) can be written as an integral over $(0, \infty)$ for which the Laguerre expansion is valid. That is, (20) can be written as

$$p_{E_n}(x) = \int_0^\infty \{ p_W[x - \rho(y - q_N(y))] + p_W[x + \rho(y - q_N(y))] \} p_{E_{n-1}}(y)\, dy. \quad (44)$$

Now expanding $p_{E_{n-1}}(y)$ by means of (42a) yields

$$p_{E_n}(x) = \sum_{k=0}^{\infty} \beta_k^{(n-1)} \int_0^\infty \{ [p_W[x - \rho(y - q_n(y))] + p_W[x + \rho(y - q_N(y))] \} l(y) L_k(y)\, dy, \quad (45)$$

and again using (42d) implies

$$\beta_l^{(n)} = \sum_{k=0}^{\infty} B_{l,k} \beta_k^{(n-1)}, \qquad l = 0, 1, \cdots, \quad (46a)$$

where

$$B_{l,k} = \int_0^\infty \int_0^\infty \{ p_W[x - \rho(y - q_N(y))] + p_W[x + \rho(y - q_N(y))] \} \cdot l(y) L_l(x) L_k(y)\, dx dy, \quad l, k = 0, 1, \cdots. \quad (46b)$$

Equation (46a), analogous to (38a) for the Hermite series expansions, provides the recursive formula for updating the Laguerre series expansion coefficients. In Appendix B a simplification of the double integral in (45b) is given.

In the following section, we will use the algorithmic procedures described in Section IV and the above expansion methods to investigate the optimum performance of DPCM schemes operating upon first-order Gauss–Markov and Laplace–Markov processes.

VI. Numerical Results

In this section we present numerical results describing the rate-distortion performance of optimum DPCM schemes driven by first-order Gauss–Markov and Laplace–Markov processes.

At the outset, note that in all these results the quantizer is taken to be a *uniform-threshold quantizer*. A uniform threshold quantizer is described by $T_{l+1} - T_l = \delta\sigma_E$, $l = 1, 2, \cdots, N - 2$, where δ is the step size normalized to the standard deviation of the prediction error. The normalized width of the outer intervals is η so that $\delta\sigma_E = [(T_N - T_0) - 2\eta\sigma_E]/(N - 2)$. For $\delta = 0$, the quantizer becomes a two-level symmetric quantizer, cf. [13]. This restriction is imposed because of the complexity associated with the algorithmic methods used for designing optimal entropy-constrained quantizers driven by memoryless sources. These algorithms must be used in step 3) of either Algorithm 1 or Algorithm 2 of Section IV. While imposing uniformity on the quantizer threshold levels results in a suboptimal system, it reduces the complexity of the quantizer design procedure considerably [13].

In all cases, the quantizer is chosen to be symmetric. Since the input distributions under study are also symmetric, for reasons described in [13], the number of quantization levels is taken to be odd. In particular, this assumption enables achievement of rates below 1 b/sample.

A. Rate-Distortion Performance Results

Algorithms 1 and 2, along with the polynomial expansions of Section V, are used to obtain the optimal rate-distortion theoretic performance of DPCM employing uniform-threshold quantizers, operating on Gauss–Markov and Laplace–Markov sources. In all cases (described below) the two algorithms converged to the same quantizer and hence yielded exactly the same result.

Performance curves for different values of the correlation coefficient ρ (i.e., different amounts of memory in the source) have been obtained. Results for $\rho = 0.2$, 0.5, and -0.8 for $N = 3, 5, 9$, and in some cases 17 and 33, are illustrated in Figs. 3–5 and 6–8 for Gaussian and Laplacian sources, respectively. In all cases we have normalized the mean-square distortion D to the source variance σ_x^2. In Figs. 3–5 we have included the rate-distortion function $R(D)$ of the corresponding Gauss-Markov source. For Laplace–Markov sources, since effective means for computing the rate-distortion function are not available, upper and lower bounds ($R_U(D)$, and $R_L(D)$, respectively) for the rate-distortion function are developed and illustrated in Figs. 6–8. Furthermore, asymptotic results for the rate-distortion performance of such schemes at high rates and for a large number of quantization levels are included in all performance curves. This asymptotic result is simply an extension of the Gish-Pierce asymptote for zero-memory quantization of memoryless sources [29]. These rate-distor-

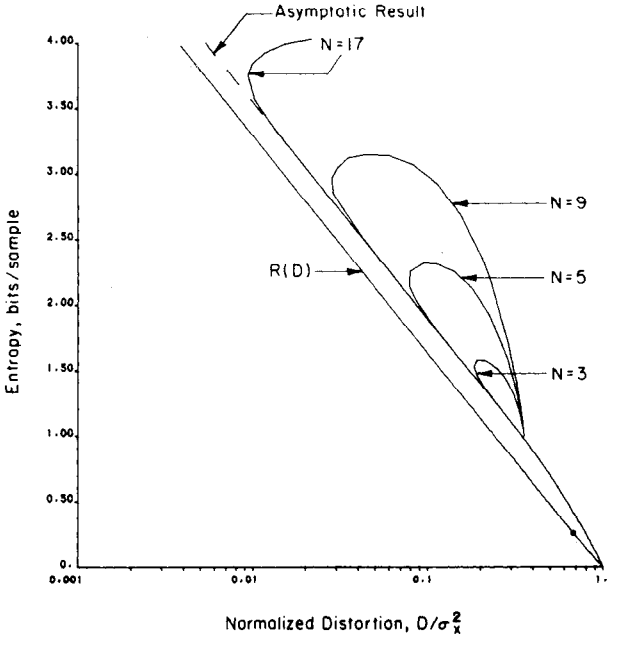

Fig. 3. Performance of optimum DPCM coding scheme for first-order Gauss–Markov source with $\rho = 0.2$.

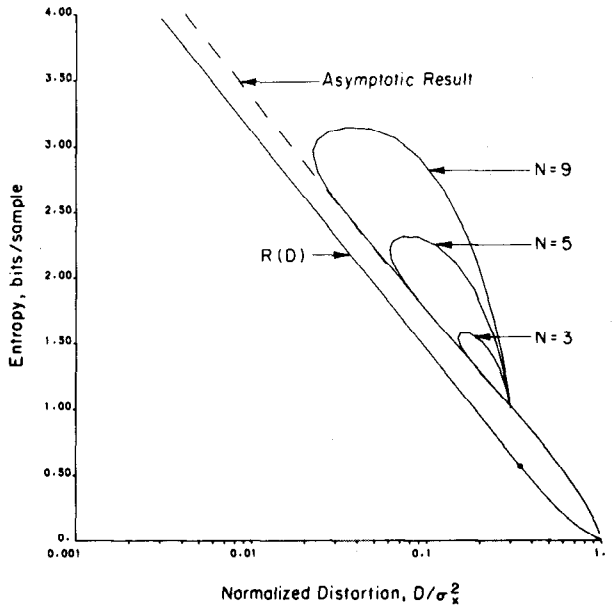

Fig. 4. Performance of optimum DPCM coding scheme for first-order Gauss–Markov source with $\rho = 0.5$.

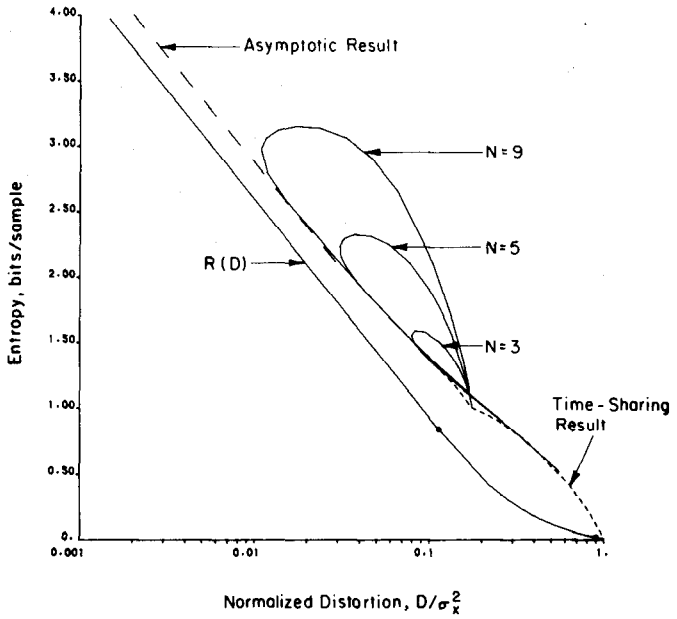

Fig. 5. Performance of optimum DPCM coding scheme for first-order Gauss–Markov source with $\rho = 0.8$.

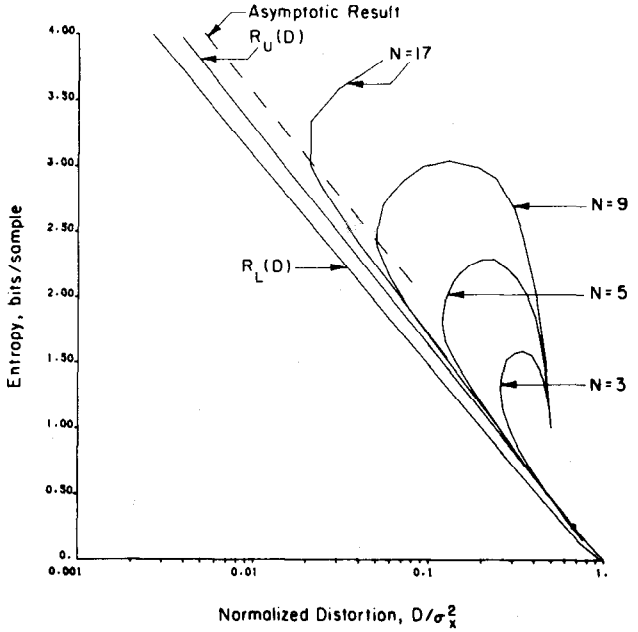

Fig. 6. Performance of optimum DPCM coding scheme for first-order Laplace–Markov source with $\rho = 0.2$.

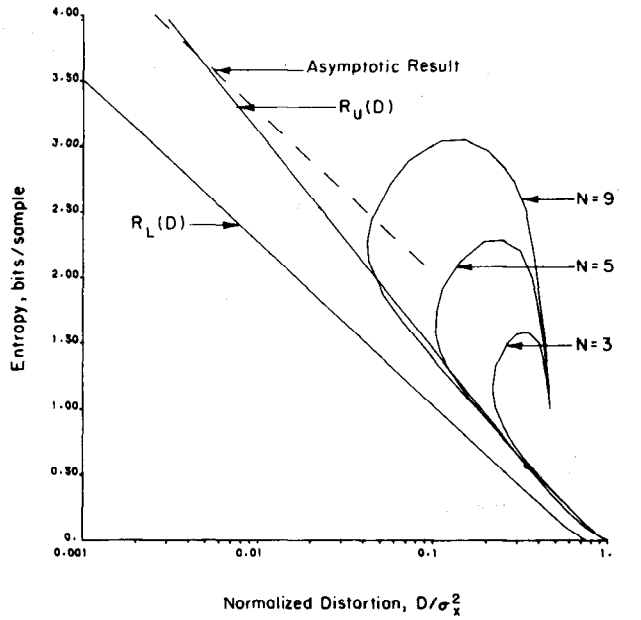

Fig. 7. Performance of optimum DPCM coding scheme for first-order Laplace–Markov source with $\rho = 0.5$.

tion function bounds and asymptotic performance results are discussed in the next section.

Let us note that for both Gauss–Markov and Laplace–Markov sources, for rates in excess of 1 b/sample, we have obtained two quantizers satisfying the necessary conditions. Clearly, for the same value of output entropy, the optimum performance is obtained by the quantizer yielding the smaller distortion. Thus, in Figs. 3–8 the optimum performance is determined by the lower envelope of the performance curves corresponding to different number of quantization levels. Nevertheless, for reasons that will become clear shortly, we have in most cases included the upper portion of the performance curves as well.[6]

Several comments about the performance curves are in order. In Figs. 3–5 (Gauss–Markov source), the asymptotic results agrees favorably with our numerical result even at relatively low rates. This agreement is more pronounced at low correlation values. Moreover, similar to the memoryless situation [29], there is only a 0.255 b/sample dif-

[6]The exception here is the case $N = 17$ where the upper portion of these curves is not shown to simplify the figures.

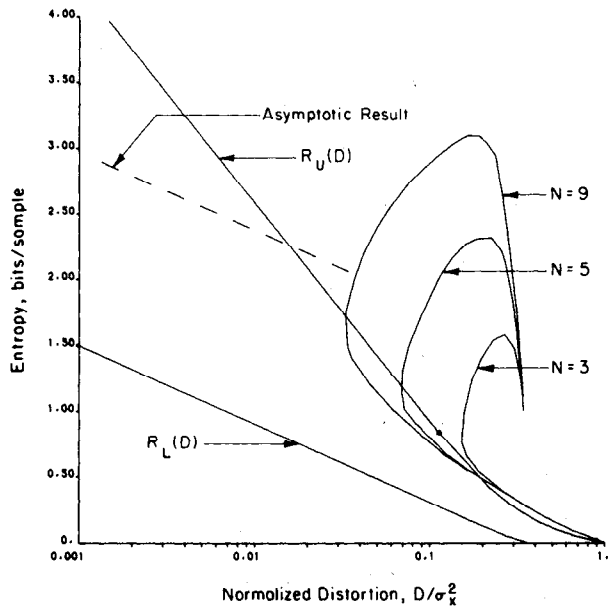

Fig. 8. Performance of optimum DPCM coding scheme for first-order Laplace–Markov source with $\rho = 0.8$.

ference between the performance of the optimum DPCM quantizer and the rate-distortion function at high rates. We shall elaborate on this in the next section.

It can be seen from Figs. 3 and 4 that for low values of ρ the difference between the performance of the DPCM system and the rate-distortion function becomes smaller for decreasing rates. For larger values of ρ, however, this difference becomes larger at low rates. Specifically, the maximum difference for $\rho = 0.8$ is observed to be about 0.55 b/sample. This implies that DPCM quantization schemes are relatively less efficient at low rates when the source is highly correlated.

For Laplace–Markov sources our results demonstrate similar behavior. Here, the difficulty is that the performance curves (especially at high correlation values) approach the asymptotic result very slowly. For reasons to be described, obtaining the rate-distortion performance of the DPCM quantizer at high rates and large number of quantization levels becomes exceedingly difficult at high correlation values. Therefore, for large ρ our performance curves, in the Laplace–Markov case, do not demonstrate the validity of the asymptotic result. Nevertheless, results in Fig. 6 for $\rho = 0.2$ indicate slow convergence of the performance curves to the asymptotic result with increasing N. For $\rho = 0$, a more rapidly converging set of results is reported in [12].

Finally, let us note that in the Laplacian case the difference between the rate-distortion function lower bound and the asymptotic result for high rates is no longer equal to 0.255 b/sample. The exact value of this difference is calculated in the next section. At low rates, nevertheless, the optimum performance curve is very close to the rate-distortion function lower bound. However, the number of quantization levels plays a more important role, in the sense that a relatively larger number (compared to the Gaussian case) of quantization levels is required to obtain the optimum performance. For example, for the Laplace-Markov source with $\rho = 0.5$ at 1 b/sample an additional 1-dB in signal-to-noise ratio (S/N) can be gained by increasing the number of levels from three to nine.

B. Comparison with Two-Level Schemes

Note that the limiting form of a three-level symmetric uniform-threshold quantizer as the step size δ approaches zero is a two-level (binary) symmetric quantizer. In all our results, for three-level schemes at 1 b/sample we have obtained two quantizers satisfying the necessary conditions, one of which is the above binary quantizer. The rate-distortion performance of the system with this binary quantizer is determined by the endpoint of the three-level performance curves at one b/sample.

Binary predictive quantization schemes (sometimes called delta modulation) play an important role in data compression for their ease of implementation. Arnstein [5] has studied the optimum performance of such systems for Gaussian autoregressive inputs. The following discussion provides further insight concerning the performance of such systems and the potential advantages of a system with additional quantization levels.

First, note that for Gauss–Markov sources no tangible improvement at 1 b/sample is obtained by increasing the number of levels from three to five or even nine. Therefore, for Gaussian sources, the optimum performance at 1 b/sample can be achieved by at most three quantization levels. For small correlation values ($\rho = 0$, and 0.2), the three-level scheme offers a slight improvement over the binary scheme. For higher correlation values ($\rho = 0.5$ and 0.8), interestingly, the opposite behavior is observed. That is, the optimum two-level scheme outperforms the three-level one. It must be kept in mind, however, that we have confined attention to symmetric uniform-threshold schemes. When this restriction is removed, performance at least as good as a two-level system can be obtained. Finally, it should be mentioned that the nonconvex behavior of the performance curve for $\rho = 0.8$ at low rates (Fig. 5) can be convexified by a time-sharing of appropriate quantizers [30]. The dotted line in Fig. 5 designates this time-sharing result. In Table I we have summarized the rate-distortion performance of the optimal two-level and

TABLE I
S / N OF OPTIMUM DPCM CODING SCHEMES AND COMPARISON WITH RATE-DISTORTION FUNCTION AT 1 B / SAMPLE FOR STATIONARY GAUSS–MARKOV SOURCES

ρ	2-level	3-level	$R(D)$
0.0	4.39 dB	4.59 dB	6.02 dB
0.2	4.51	4.65	6.20
0.5	5.22	5.09	7.27
0.8	7.56	6.85	10.46

TABLE II
S / N OF OPTIMUM DPCM CODING SCHEMES AND COMPARISON WITH RATE-DISTORTION FUNCTION BOUNDS AT 1 B / SAMPLE FOR STATIONARY LAPLACE–MARKOV SOURCES

ρ	2-level	3-level	5-level	9-level	$R_L(D)$	$R_U(D)$
0.0	3.01 dB	5.23 dB	5.75 dB	5.76 dB	6.62 dB	6.02 dB
0.2	3.03	5.40	5.98	6.00	6.97	6.20
0.5	3.36	6.44	7.42	7.50	9.81	7.27
0.8	4.65	8.00	11.14	11.80	21.69	10.46

three-level symmetric systems, as well as the corresponding values of the rate-distortion function at 1 b/sample (including the $\rho = 0$ case).

For Laplace–Markov sources the results are quite different. In all cases, the optimum three-level scheme outperforms the binary scheme at 1 b/sample. The rationale for such behavior is easily explained. Due to the impulse component in the pdf of $\{W_n\}$ (cf. (41b)), the prediction error assumes values close to zero with very high probability, and hence any symmetric binary scheme fails to be efficient since it does not include a representative zero level. (Specific examples of symmetric sources with high probabilities about the origin are given in [37]. It is shown that symmetric two-level quantizers are not optimal for these sources.) Moreover, as one can see from the performance curves in Figs. 6–8, further improvement can be obtained by increasing the number of quantization levels. Again, a summary of results (including the $\rho = 0$ case) for different number of quantization levels and the corresponding rate-distortion function bounds for the Laplace–Markov source are presented in Table II. For example, at $\rho = 0.8$ an improvement in excess of 7 dB in S/N can be achieved by going from a two-level to a nine-level quantizer.

C. Convergence and Uniqueness

It can be observed from Figs. 3–8 that the solution to the necessary conditions for optimality is nonunique for output entropies in excess of 1 b/sample. Specifically, for $1 \le H_0 < \log_2 N$ there exist two couples (q_N, p_E) satisfying Conditions 1 and 2 of Section III. From a rate-distortion standpoint, only that solution yielding the smaller distortion (lower portion of the performance curve) is useful. However, to demonstrate the nonunique nature of the solution and, more importantly, to study the behavior of the binary quantizer situation, we have in most cases included all these results, including nonoptimum ones, in our performance curves.

As mentioned earlier, in all cases the two algorithms described in Section IV converged to the same optimum quantizer. The major difficulty in implementing these algorithms is computing the coefficients of the series expansion for the prediction error pdf. Recall that, in theory, an infinite matrix multiplication operation described by (38a) and (46a) is necessary to compute the steady-state expansion coefficients. In a practical situation, however, we are forced to use a truncated version of (38a) or (46a). This raises the question of whether the truncated version includes enough terms for an accurate computation of the coefficients. In what follows we shall elaborate on this.

First, note that a standard (i.e., zero-mean, unit-variance) normal density can be described by the Gram–Charlier expansion with $\alpha_0 = 1$, and $\alpha_k = 0$, $k \ge 1$. We say then that the series expansion of (35a) is "matched" to a standard normal density. Thus, it is possible to express a pdf close to standard normal by means of the Gram–Charlier expansion with a small number of coefficients. Indeed, this has been the case for the pdf of the prediction error at high rates. (At high rates, where the quantization error is small, we have $E_n \approx W_n$, and hence E_n has a density close to the standard normal.) In fact, for the Gauss–Markov source with $\rho = 0.8$, as Arnstein [5] correctly points out, even at rates as low as 1 b/sample a small number of coefficients provide sufficient accuracy. In Tables III and IV, for $H_0 = 1$ b/sample we have presented the steady-state expansion coefficients describing the pdf

TABLE III
STEADY-STATE HERMITE POLYNOMIAL EXPANSION COEFFICIENTS FOR A TWO-LEVEL OPTIMAL SYSTEM DRIVEN BY A STATIONARY GAUSS–MARKOV SOURCE WITH $\rho = 0.8$[a]

$\alpha_0 = 1.000000$	
$\alpha_2 = 0.155708$	
$\alpha_4 = 0.226487$	E-01
$\alpha_6 = 0.253093$	E-02
$\alpha_8 = 0.231255$	E-03
$\alpha_{10} = 0.180370$	E-04
$\alpha_{12} = 0.123977$	E-05
$\alpha_{14} = 0.767338$	E-07
$\alpha_{16} = 0.433662$	E-08
$\alpha_{18} = 0.225994$	E-09
$\alpha_{20} = 0.109315$	E-10
$\alpha_{2k+1} = 0, \quad k0, 1, \cdots$	

[a] $N = 2$, $T_1 = 0$, $Q_1 = -Q_2 = 0.9081$. Normalized Distortion = 0.17508; output entropy = 1.00.

TABLE IV
STEADY-STATE HERMITE POLYNOMIAL EXPANSION COEFFICIENTS FOR A THREE-LEVEL UNIFORM THRESHOLD OPTIMAL SYSTEM DRIVEN BY A STATIONARY GAUSS–MARKOV SOURCE WITH $\rho = 0.8$[a]

$\alpha_0 = 1.000000$	
$\alpha_2 = 0.180650$	
$\alpha_4 = 0.277711$	E-01
$\alpha_6 = 0.294607$	E-02
$\alpha_8 = 0.234260$	E-03
$\alpha_{10} = 0.144731$	E-04
$\alpha_{12} = 0.714309$	E-06
$\alpha_{14} = 0.288450$	E-07
$\alpha_{16} = 0.973740$	E-09
$\alpha_{18} = 0.280507$	E-10
$\alpha_{20} = 0.704617$	E-12
$\alpha_{2k-1} = 0, \quad k = 0, 1, \cdots$	

[a] $N = 3$, $T_2 = -T_1 = 1.3850$, $Q_3 = -Q_1 = 1.9736$, $Q_2 = 0$. Normalized Distortion = 0.20323; output entropy = 1.0096.

of the prediction error when the source is Gauss–Markov with $\rho = 0.8$ and the quantizers are the optimum two and three-level quantizer, respectively. Note that our results for the binary quantizer agree with Arnstein's [5]. In all cases, we have taken the number of coefficients large enough so that no discernable change in the results can be achieved by any further increase.

At low rates, the variance of the prediction error increases. In fact, in the extreme case of $H_0 = 0$, $\sigma_E^2 = 1/(1 - \rho^2)$. (This occurs when the middle quantization interval occupies the entire support of the prediction error pdf. In this case $Y_n = 0$ and hence $E_n = X_n$.) Therefore, for $|\rho|$ close to one, σ_E^2 becomes very large and hence the prediction error pdf deviates considerably from the standard normal density. Therefore, in the low-rate regime, a larger number of coefficients is required. Indeed, for $\rho = 0.8$ we had to use 56 coefficients in the expansion of the prediction error pdf for $H_0 = 0.53$ b/sample. This has been the lowest rate for which we were able to obtain the optimum performance for $\rho = 0.8$.

For Laplace–Markov sources the situation is slightly different. The series expansion based on Laguerre polynomials given in (42a) is matched to a Laplacian density described by (40a). Therefore, a pdf close to Laplacian can be expressed by (42a) with a small number of coefficients. This is the case for the pdf of the prediction error when the output entropy is small. More specifically, $E_n \approx X_n$ so that $p_E(\cdot)$ is close to that given by (40a). At higher rates, where the pdf of the prediction error deviates from a Laplacian density, a larger number of coefficients is required. This has been the major difficulty in obtaining the rate-distortion performance of the DPCM quantization scheme driven by Laplace–Markov sources at high rates.

VII. Asymptotic Results and Bounds

Let us assume that an optimal DPCM coding scheme with entropy constraint H_0 is designed, and let $p_E^*(\cdot)$ denote the steady-state marginal pdf of the prediction error sequence. If the prediction error exhibits a certain degree of smoothness, the asymptotic result developed by Gish and Pierce [29] determines the rate-distortion performance of the optimum quantizer at high rates. Specifically, if the number of quantization levels N is large and if the output entropy H_0 is also large (low distortion), then the average quantization error D is given by

$$D = \frac{1}{12} 2^{2(h_E^* - H_0)}, \tag{47}$$

where h_E^* is the differential entropy of a memoryless source with pdf $p_E^*(\cdot)$.

It is the intent of this section to develop similar asymptotic formulas for the performance of DPCM encoding schemes at high rates and make appropriate comparisons with the rate-distortion function lower bound for both Gauss–Markov and Laplace–Markov sources. The following theorem proves useful in the development.

Theorem 3: Let $R_X(D)$ and $R_E(D)$ be the rate-distortion functions (subject to a squared-error distortion measure) of the input process $\{X_n\}$ and the prediction error process $\{E_n\}$, respectively. Then there is a critical distortion $D_c^* > 0$ such that

$$R_X(D) = R_E(D), \qquad D \in (0, D_c^*].$$

Proof: For convenience we assumed $M = 1$. Then (11a) and (11b) yield

$$\hat{X}_n = Y_n + \sum_{i=1}^{n-1} \rho^i Y_{n-i}, \qquad n = 1, 2, \cdots, \tag{48}$$

and hence

$$X_n = E_n + \sum_{i=1}^{n-1} \rho^i q_N(E_{n-i}), \qquad n = 1, 2, \cdots. \tag{49}$$

Now if we define $\boldsymbol{X}^N$ and $\boldsymbol{E}^N$ as in Theorem 2, we can write

$$\boldsymbol{X}^N = F_N(\boldsymbol{E}^N), \tag{50}$$

where F_N is a nonlinear operator. Letting J_{F_N} define the Jacobian of this transformation, we have

$$J_{F_N} = \det\left[\frac{\partial X_i}{\partial E_j}\right]. \tag{51}$$

It is easily shown that the Jacobian matrix is a lower triangular matrix with diagonal entries equal to one. Thus

$$J_{F_N} = 1. \tag{52}$$

Conversely, we can write

$$\boldsymbol{E}^N = F_N^{-1}(\boldsymbol{X}^N), \tag{53}$$

where F_N^{-1} is the inverse of F_N. Here, again we can show that the Jacobian of F_N^{-1} is unity, i.e.,

$$J_{F_N^{-1}} = 1. \tag{54}$$

Now we resort to a Theorem by Hopkins [31, Theorem 2.2] in which it is established that

$$R_X(D) \geq R_E(D) - \sum \lim_{N \to \infty} \frac{1}{N} \int_{R^N} p_E^N(e) \log |J_{F_N}| \, de, \tag{55}$$

for $D \in (0, D_{c_1}^*]$, where $D_{c_1}^* > 0$ and $p_E^N(\cdot)$ is the N-fold pdf of the prediction error sequence. Using (52) we can write the last inequality as

$$R_X(D) \geq R_E(D), \qquad D \in (0, D_{c_1}^*]. \tag{56}$$

Interchanging the roles of X and E and using (54), we will have

$$R_E(D) \geq R_X(D), \qquad D \in (0, D_{c_2}^*], \tag{57}$$

where $D_{c_2}^* > 0$. Now comparing (56) and (57) yields

$$R_X(D) = R_E(D), \qquad D \in (0, D_c^*], \tag{58}$$

where $D_c^* = \min\{D_{c_1}^*, D_{c_2}^*\} > 0$, which was to be proved.

This theorem, in effect, substantiates the fact that at high rates the rate-distortion function of the source and prediction error coincide. This is not surprising, however, since at high rates the prediction error is very close to the innovation sequence $\{W_n\}$ generating the input autoregressive process and it is established by Gray [32] for Gaussian autoregressive processes, and by Hopkins [31] for a generic autoregressive process, that there is a critical distortion D_c below which the rate-distortion functions of the source $\{X_n\}$ and the innovation sequence $\{W_n\}$ coincide.

In general, we conjecture that the rate-distortion function of the prediction error is upper bounded by the source rate-distortion function and lower bounded by the innovation sequence rate-distortion function. This is based on the argument that when the quantizer is very fine so that $q_N(x) = x$, E_n equals W_n and hence $R_E(D) = R_W(D)$. On the other hand, when the quantizer is very coarse so that $q_N(x) = 0$, $\forall x$, $E_n = X_n$ and thus $R_E(D) = R_X(D)$. In intermediate cases, we suspect $R_W(D) \le R_E(D) \le R_X(D)$. This conjecture remains to be proved. At high rates (i.e., $D \le \min\{D_c^*, D_c\}$), however, we do have

$$R_W(D) = R_E(D) = R_X(D). \tag{59}$$

A. Asymptotic Results

For the Gauss–Markov case, at high rates the prediction error possesses a normal density for which the Gish–Pierce asymptote is valid, as given by (47), with

$$h_E^* = \frac{1}{2}\log_2 2\pi e\sigma_E^2. \tag{60}$$

But from (28), we have

$$\sigma_E^2 = \sigma_W^2 + \rho^2 D. \tag{61}$$

Thus, (47) can be written as

$$D = \frac{(\pi e/6)\sigma_W^2 2^{-2H_0}}{1-(\pi e/6)\rho^2 2^{-2H_0}} \triangleq \hat{D}(H_0), \tag{62}$$

which determines the asymptotic behavior of the system at high rates. Notice that for H_0 sufficiently large we have

$$\hat{D}(H_0) \simeq (\pi e/6)\sigma_W^2 2^{-2H_0}, \tag{63a}$$

or, correspondingly,

$$H_0 = \frac{1}{2}\log_2(\pi e/6) + \frac{1}{2}\log_2\left(\sigma_W^2/D\right). \tag{63b}$$

This asserts that at high rates there is a $(1/2)\log_2(\pi e/6) \approx 0.255$ b/sample difference between $R_W(D) = R_X(D)$ and the asymptotic result. This, of course, conforms with the previously reported results in [9] and [33].

For the Laplace–Markov source this situation is totally different. This is mainly due to the fact that the Gish–Pierce result [29] requires a certain degree of smoothness in the source density. This, unfortunately, is not the case here due to the impulse component in (41b). In the following we provide some discussion of this subtle issue.

Let us consider a memoryless source whose pdf is described by (41b). We want to obtain asymptotic results for the quantizer performance in this case. We assume that the point $x = 0$ is not the boundary of any two quantization intervals. This is because the point $x = 0$ occurs with a highly probability and, hence, assigning an appropriate representative level will help reduce the average distortion. We, moreover, assume that the point $x = 0$ belongs to the i^*th quantization interval and $Q_{i^*} = 0$. Then the probability of the ith quantization level is given by

$$P_i = \begin{cases} (1-\rho^2)P_i', & i \ne i^* \\ \rho^2 + (1-\rho^2)P_{i^*}', & i = i^*, \end{cases} \tag{64}$$

where P_i' is the corresponding probability of the ith quantization level when $\rho = 0$ in (41b).

The quantizer output entropy is then given by

$$H_0 = -\left[\rho^2 + (1-\rho^2)P_{i^*}'\right]\log_2\left[\rho^2 + (1-\rho^2)P_{i^*}'\right] - \sum_{i \ne i^*}(1-\rho^2)P_i'\log_2\left[(1-\rho^2)P_i'\right], \tag{65}$$

which can be simplified to

$$H_0 = (1-\rho^2)H_0' - \rho^2\log_2\left[\rho^2 + (1-\rho^2)P_{i^*}'\right] - (1-\rho^2)\log_2(1-\rho^2) + (1-\rho^2)P_{i^*}' \cdot \log_2\frac{(1-\rho^2)P_{i^*}'}{\rho^2 - (1-\rho^2)P_{i^*}'}, \tag{66}$$

where H_0' is the quantizer output entropy when $\rho = 0$. Furthermore, the average distortion can easily be shown to be

$$D = (1-\rho^2)D', \tag{67}$$

with D' denoting the average distortion when $\rho = 0$.

In the limiting case of fine quantization (where the Gish–Pierce result holds) we have $P_{i^*}' \simeq 0$, and therefore,

$$H_0 = (1-\rho^2)H_0' + \mathscr{H}(\rho^2), \tag{68}$$

where $\mathscr{H}(\cdot)$ is the binary entropy function given by

$$\mathscr{H}(\alpha) = -\alpha\log_2\alpha - (1-\alpha)\log_2(1-\alpha), \qquad 0 \le \alpha \le 1. \tag{69}$$

When $\rho = 0$ the Gish–Pierce result holds and we have

$$D' = \frac{1}{12}2^{2(h_L - H_0')}, \tag{70}$$

in which h_L is the differential entropy of the memoryless Laplacian source in (40a). Combining (67), (68), and (70) yields

$$D = \frac{1-\rho^2}{12}2^{2(h_L - (H_0 - \mathscr{H}(\rho^2))/(1-\rho^2))}, \tag{71}$$

which is the desired result. Note that a similar result holds for the general case in which the source density is a mixture of any smooth density and an impulse, provided that h_L in (71) is replaced by the differential entropy of the smooth component.

Carter and Neuhoff [34] have developed bounding techniques for the rate-distortion function of regenerative composite sources similar to that in (41b). Specifically, if the

source density $p(\cdot)$ is described by

$$p(x) = \rho^2 p_1(x) + (1-\rho^2)p_2(x), \tag{72}$$

then the rate-distortion function is lower-bounded according to

$$R(D) \geq \inf_{D_1, D_2 \in \mathcal{D}} \{\rho^2 R_1(D_1) + (1-\rho^2)R_2(D_2)\}, \tag{73a}$$

where $R_1(\cdot)$ and $R_2(\cdot)$ are the rate-distortion functions of $p_1(\cdot)$ and $p_2(\cdot)$, respectively, and

$$\mathcal{D} = \{(D_1, D_2): \rho^2 D_1 + (1-\rho^2)D_2 \leq D\}. \tag{73b}$$

When $p_1(x) = \delta(x)$, which is the case in (41b), we have $R_1(D_1) = 0$, and hence the infimum in (73a) occurs at $D_2 = D/(1-\rho^2)$. Thus

$$R(D) \geq (1-\rho^2)R_2\left(\frac{D}{1-\rho^2}\right) \triangleq \boldsymbol{R}(D). \tag{74}$$

Using the Shannon lower bound [28], which is tight at high rates, for $R_2(\cdot)$ in (74) we can write

$$\boldsymbol{R}(D) \geq (1-\rho^2)\left[h_L - \frac{1}{2}\log_2 \frac{2\pi e D}{1-\rho^2}\right]. \tag{75}$$

From (71) we have

$$H_0 = \mathcal{H}(\rho^2) + (1-\rho^2)\left[h_L - \frac{1}{2}\log_2 \frac{12D}{1-\rho^2}\right], \tag{76}$$

which enables us to determine the difference between the rate-distortion function lower bound $\boldsymbol{R}(D)$ and the asymptotic performance expressed by (76). Unlike the Gish–Pierce result we get[7]

$$\begin{aligned}\Delta R &\triangleq H_0 - \boldsymbol{R}(D) = \mathcal{H}(\rho^2) + \frac{1-\rho^2}{2}\log_2 \frac{\pi e}{6} \\ &= \mathcal{H}(\rho^2) + (1-\rho^2)0.255, \text{ b/sample.}\end{aligned} \tag{77}$$

Envision the memoryless source of (41b) as the output of a switch that randomly and independently moves between two positions: up and down. The switch is up with probability ρ^2 and down with probability $(1-\rho^2)$. When the switch is up its output is zero with probability one. When the switch is down its output is a real-valued variable distributed according to (40a). With this in mind an interesting interpretation for (77) can be provided. The quantization performance penalty is a factor $(1-\rho^2)$ of the ordinary penalty 0.255 b/sample plus an additional term equal to the uncertainty in the switch position.

Note that, as one would expect, for $\rho = 0$, $\mathcal{H}(0) = 0$, and $\Delta R = 0.255$ b/sample. On the other hand, for $\rho = 1$, $\Delta R = 0$. This makes sense, for at $\rho = 1$ the source output is zero with probability one and there is no uncertainty in the switch position. Straightforward differentiation implies that ΔR is maximized at

$$\rho = \frac{1}{\sqrt{1+\sqrt{\pi e/6}}} \simeq 0.675 \tag{78}$$

and that $\Delta R_{\max} = \log_2(1+\sqrt{\pi e/6}) \simeq 1.133$ b/sample.

[7]We conjecture that $R(D)$ in (74) is tight. If this conjecture is true, the quantity ΔR is truly representative of the penalty due to zero-memory quantization of the source given by (72).

Now we are in a position to determine the asymptotic performance of the DPCM coding scheme driven by Laplace–Markov sources. We assume that at high rates the pdf of the error sequence is close to that of the innovation sequence. Thus using (71), we can write

$$D = \frac{1-\rho^2}{12} 2^{2(h_L^* - (H_0 - \mathcal{H}(\rho^2))/(1-\rho^2))}, \tag{79}$$

where h_L^* is the differential entropy of the smooth component in the pdf of the prediction error. This quantity can easily be shown to be

$$h_L^* = 1 + \log_2 \frac{e\sigma_E}{\sigma_W} \quad \text{b/sample.} \tag{80}$$

Again, using (61), we can write the asymptotic performance as

$$\begin{aligned}D &= \frac{((1-\rho^2)e^2/3)2^{-2(H_0 - \mathcal{H}(\rho^2))/(1-\rho^2)}}{1 - ((1-\rho^2)e^2\rho^2/3\sigma_W^2)2^{-2(H_0 - \mathcal{H}(\rho^2))/(1-\rho^2)}} \\ &\triangleq \hat{D}(H_0).\end{aligned} \tag{81}$$

For sufficiently large H_0, (81) can be approximated by

$$\hat{D}(H_0) \simeq ((1-\rho^2)e^2/3)2^{-2(H_0 - \mathcal{H}(\rho^2))/(1-\rho^2)}, \tag{82}$$

or, equivalently,

$$H_0 = \mathcal{H}(\rho^2) + \frac{1-\rho^2}{2}\log_2 \frac{(1-\rho^2)e^2}{3D}. \tag{83}$$

Comparing (83) to $\boldsymbol{R}(D)$ in (75), which is also a tight lower bound to $R_X(D)$ at high rates, results in a difference equal to that given in (77), as one would expect.

Asymptotic results illustrated in Figs. 3–5 and 6–8 are obtained by means of (62) and (81), respectively.

B. Rate-Distortion Function Bounds

For the Gaussian case the rate-distortion function can be calculated exactly [28], [32]. For the Laplacian case, for which the rate-distortion function is not known exactly, we have used upper and lower bounds. The upper bound is the well-known Gaussian upper bound [28] and the lower bound is the autoregressive lower bound [32]. This lower bound is determined in terms of the rate-distortion function of the innovation sequence described by (41b). This rate-distortion function, in turn, has been lower bounded by the Carter–Neuhoff composite lower bound described in (74). (In Figs 3–8 the Gaussian upper bound and the combined autoregressive composite lower bound are designated by $R_U(D)$ and $R_L(D)$, respectively.) We have used the Blahut algorithm [35] for computing $R_2(\cdot)$ in (74).

VIII. Summary and Conclusions

We have studied the structural properties of optimum DPCM schemes for Mth-order autoregressive inputs. Necessary conditions for optimality of the quantizer in these schemes are developed and algorithmic approaches for designing such quantizers are proposed. Also, difficulties inherent in computing the distribution of the prediction

error are examined carefully. To overcome these problems, we have developed series expansion methods matched to the source distribution. Our algorithmic procedures for optimum quantizer design are used in conjunction with the series expansion techniques to design optimum uniform-threshold entropy-constrained DPCM encoding schemes for first-order Gaussian and Laplacian autoregressive sources. It is shown that for Gaussian sources there could be a wide gap between the optimum performance and the rate distortion function at low rates, when the source is highly correlated.

Asymptotic results, similar to those developed by Gish and Pierce [29] in the memoryless case, are developed in some detail. These results, which agree favorably with our numerical results in the Gaussian case, imply that at high rates there is only a 0.255-b/sample performance penalty. Corresponding asymptotic results for Laplacian sources demonstrate a wider gap between the optimum quantizer performance and the rate-distortion function lower bound. Unfortunately, at high correlation values our numerical results in the Laplacian case are not sufficient to demonstrate the validity of the predicted asymptotic performance. Because of the complexity of the quantizer design procedure at high rates when the number of levels is large, we were not able to provide performance results beyond $N = 17$.

In all our numerical results we have restricted attention to uniform-threshold quantizers. Obviously, removal of this constraint can only improve the performance. We have decided to forego studying this issue, however, because of the complexity of more general optimum entropy-constrained quantizer design procedures.

A logical extension of this research is to consider the case $\rho = 1$. Indeed, (1) with $M = 1$, $\rho = 1$ and Gaussian innovations represents the discrete-time version of the well-known Wiener process [6]. In this case the prediction-error density can be calculated explicitly, and hence there is no need for the series expansions. Another issue that remains to be thoroughly studied is a proof for the convergence of the algorithm as well as sufficient conditions for the quantizer optimality.

Finally, we should note that we have considered only the first-order entropy of the quantizer output. At low rates, the prediction error is highly correlated and hence the entropy rate at the quantizer output might be noticeably lower than the first-order entropy. Computing or bounding this entropy rate is another issue that deserves study.

Acknowledgment

The authors would like to express their appreciation to Professor E. Masry of the University of California, San Diego, for helpful comments in the early stages of this work. They would like also to acknowledge the comments of the reviewers which helped to improve an earlier version of this paper.

Appendix A
Recursive Equation for Updating the Hermite Expansion Coefficients

In this appendix we present a simplified version of (38b) in the text. Also, formulas describing the quantizer output entropy and average distortion in terms of the Hermite expansion coefficients will be given.

Let us define

$$F_l(y) \triangleq \int_{-\infty}^{\infty} P_W[x - \rho(y - q_N(y))]\, H_l(x)\, dx, \qquad l = 0, 1, \cdots. \quad \text{(A.1)}$$

Then, replacing $p_W(x)$ by $g(x)$ and using (35c), it is easy to show that

$$F_l(y) = \rho^l [y - q_N(y)]^l, \qquad l = 0, 1, \cdots. \quad \text{(A.2)}$$

Thus (38b) of the text can be written as

$$A_{l,k} = \frac{\rho^l}{l!} \int_{-\infty}^{\infty} g(y)\, H_k(y) [y - q_N(y)]^l\, dy, \qquad k, l = 0, 1, \ldots. \quad \text{(A.3)}$$

Again, using (35c) and integrating by parts yields the following result:

$$A_{l,k} = \begin{cases} \dfrac{\rho^l}{(l-k)!} \displaystyle\sum_{i=1}^{N} \int_{T_{i-1}}^{T_i} (x - Q_i)^{l-k} g(x)\, dx, & l > k \\ \rho^l \left[1 - \displaystyle\sum_{i=1}^{N-1} (Q_{i+1} - Q_i)\, g(T_i) \right], & l = k \geq 1 \\ \rho^l \displaystyle\sum_{i=1}^{N-1} (Q_{i+1} - Q_i)\, H_{K-l}(T_i)\, g(T_i), & 1 \leq l \leq k, \end{cases} \quad \text{(A.4a)}$$

with

$$A_{0,0} = 1 \quad \text{(A.4b)}$$

$$A_{0,k} = 0, \quad k \geq 1. \quad \text{(A.4c)}$$

Here, as in [5], we have assumed that $q_N'(x)$ is zero everywhere except where $x - q_N(x)$ is zero, in which case $q_N'(x)$ is an impulse whose weight is equal to the quantizer jump at that point.

Using (61) and the facts that $\sigma_W^2 = 1$ and $\sigma_E^2 = 2\alpha_2 + 1$ (cf. [5]), implies

$$D = 2\frac{\alpha_2}{\rho^2}. \quad \text{(A.5)}$$

The quantizer output entropy H is given by (25), where P_l can be expressed as

$$P_l = \int_{T_{l-1}}^{T_l} P_E(x)\, dx = \sum_{k=0}^{\infty} \alpha_k \int_{T_{l-1}}^{T_l} g(x)\, H_k(x)\, dx. \quad \text{(A.6)}$$

But

$$\int_{T_{l-1}}^{T_l} g(x)\, H_k(x)\, dx = g(T_{l-1})\, H_{k-1}(T_{l-1}) - g(T_l)\, H_{k-1}(T_l), \qquad k \geq 1. \quad \text{(A.7)}$$

Thus,

$$P_l = \alpha_0 \int_{T_{l-1}}^{T_l} g(x)\,dx + \sum_{k=1}^{\infty} \alpha_k [g(T_{l-1})H_{k-1}(T_{l-1}) - g(T_l)H_{K-1}(T_l)], \quad l = 1,2,\cdots, \quad \text{(A.8)}$$

which, together with (25), leads to a formula for H_0 in terms of the expansion coefficients.

Appendix B
Recursive Equation for Updating the Laguerre Expansion Coefficients

In this appendix we present a simplification of (46b). Corresponding formulas for the output entropy and average distortion are also derived in terms of the Laguerre expansion coefficients.

Upon defining

$$G_l(y) \triangleq \int_0^{\infty} \{ p_W[x - \rho(y - q_N(y))] + p_W[x + \rho(y - q_N(y))]\} L_l(x)\,dx, \quad y \geq 0,\ l \geq 0, \quad \text{(B.1)}$$

we can write (46b) as

$$B_{l,k} = \int_0^{\infty} G_l(y)\,l(y)\,L_k(y)\,dy, \qquad l,k = 0,1,\cdots. \quad \text{(B.2)}$$

Noting that $p_W(\cdot)$ in (B.1) is given by (41b) and using (42c), the following simplified version of (B.1) can be obtained.

$$G_l(y) = \rho^2 + (1-\rho^2)2^{l-1}[1 - \exp\{-\rho|y - q_N(y)|\}] + \sum_{i=1}^{l} c_{i,l}|\rho|^i |y - q_N(y)|^i, \qquad l \geq 1,\ y \geq 0, \quad \text{(B.3a)}$$

where

$$c_{i,l} \triangleq \frac{(-1)^i}{i!}\left\{\frac{1-\rho^2}{2}\left[\binom{l-1}{i-1} + \sum_{j=0}^{l-i}\binom{l}{j}\right] + \rho^2\binom{l}{i}\right\}, \quad i = 1,2,\cdots,l. \quad \text{(B.3b)}$$

Also

$$G_0(y) = 1 \quad \text{(B.4)}$$

Equations (B.3) and (B.4) are used to facilitate the computation of $B_{l,k}$ expressed by the double integration in (46b).

Note that

$$L_0(x) = 1, \quad \text{(B.5a)}$$

$$L_1(x) = 1 - x, \quad \text{(B.5b)}$$

and

$$L_2(x) = 1 - 2x + \frac{1}{2}x^2. \quad \text{(B.5c)}$$

Therefore

$$\sigma_E^2 = 4(\beta_2 - 2\beta_1 + 1). \quad \text{(B.6)}$$

On the other hand,

$$\sigma_W^2 = 2(1 - \rho^2), \quad \text{(B.7)}$$

and thus using (A.5) implies

$$D = \frac{4(\beta_2 - 2\beta_1 + 1) - 2(1-\rho^2)}{\rho^2}. \quad \text{(B.8)}$$

Similar to (A.6), we can express P_l in terms of the Laguerre expansion coefficients by

$$P_l = \int_{T_{l-1}}^{T_l} P_E(x)\,dx = \sum_{k=0}^{\infty} \beta_k \int_{T_{l-1}}^{T_l} l(x)\,L_k(x)\,dx, \qquad l \geq \frac{N+1}{2} + 1, \quad \text{(B.9a)}$$

while for $l = (N+1)/2$

$$P_{(N+1)/2} = 2\sum_{k=0}^{\infty} \beta_k \int_0^{T_{(N+1)/2}} l(x)\,L_k(x)\,dx. \quad \text{(B.9b)}$$

But,

$$\int_{T_{l-1}}^{T_l} l(x)\,L_k(x)\,dx = \frac{1}{k!}\left[\frac{d^{k-1}}{dx^{k-1}}(x^k l(x))\right]\Big|_{T_{l-1}}^{T_l}, \quad \text{(B.10a)}$$

$$= \sum_{j=0}^{k-1} \frac{(-1)^{k-l-j}}{(k-j)!}[x^{k-j}e^{-x}]\Big|_{T_{l-1}}^{T_l}. \quad \text{(B.10b)}$$

Equation (B.10b), together with (B.9) and (25), describes the quantizer output entropy in terms of the expansion coefficients.

References

[1] J. B. O'Neal, Jr., "Signal to quantization noise ratio for differential PCM," *IEEE Trans. Commun. Technol.*, vol. COM-19, pp. 568–569, Aug. 1971.

[2] ——, "Delta-modulation quantizing noise-analytic and computer simulation results for Gaussian and television input signals," *Bell Syst. Tech. J.*, vol. 45, pp. 117–141, Jan. 1966.

[3] E. N. Protonotarios, "Slope overload noise in differential pulse code modulation systems," *Bell Syst. Tech. J.*, vol. 46, pp. 2119–2161, Nov. 1967.

[4] T. L. Fine, "The response of a particular nonlinear system with feedback to each of two random processes," *IEEE Trans. Inform. Theory*, vol. IT-14, pp. 255–264, Mar. 1968.

[5] D. S. Arnstein, "Quantization errors in predictive coders," *IEEE Trans. Commun.*, vol. COM-23, pp. 423–429, Apr. 1975.

[6] A. Hayashi, "Differential pulse code modulation of the Weiner process," *IEEE Trans. Commun.*, vol. COM-26, pp. 881–887, June 1978.

[7] ——, "Differential pulse code modulation of stationary Gaussian inputs," *IEEE Trans. Commun.*, vol. COM-26, pp. 1137–1147, Aug. 1978.

[8] E. Janardhanan, "Differential PCM systems," *IEEE Trans. Commun.*, vol. COM-27, pp. 82–93, Jan. 1979.

[9] V. R. Algazi and J. T. DeWitte, Jr., "Theoretical performance of entropy-encoded DPCM," *IEEE Trans. Commun.*, vol. COM-30, pp. 1088–1095, May 1982.

[10] R. B. Ash, *Real Analysis and Probability*. New York: Academic, 1972.

[11] E. Masry and S. Cambanis, "Delta modulation of the Weiner process," *IEEE Trans. Commun.*, vol. COM-23, pp. 1297–1300, Nov. 1975.

[12] N. Farvardin, "Rate-distortion performance of optimum entropy-constrained quantizers," Ph.D. thesis Elec. Comput., and Syst. Eng. Dept., Rensselaer Polytechnic Inst., Troy, NY, Dec. 1983.

[13] N. Farvardin and J. W. Modestino, "Optimum quantizer performance for a class of non-gaussian memoryless sources," *IEEE Trans. Inform. Theory*, vol. IT-30, pp. 485–497, May 1984.

[14] A. Gersho, "Stochastic stability of delta modulation," *Bell Syst. Tech. J.*, vol. 51, pp. 821–842, Apr. 1972.
[15] J. L. Doob, "Asymptotic properties of Markov transition probabilities," *Trans. Amer. Math. Soc.*, vol. 63, pp. 393–421, May 1948.
[16] L. H. Goldstein and B. Liu, "Deterministic stochastic stability of adaptive differential pulse code modulation," *IEEE Trans. Inform. Theory*, vol. IT-23, pp. 445–453, July 1977.
[17] J. C. Kieffer, "Stochastic stability for feedback quantization schemes," *IEEE Trans. Inform. Theory*, vol. IT-28, pp. 248–254, Mar. 1982.
[18] H. Hochstadt, *Integral Equations*. New York: Wiley, 1973.
[19] L. D. Davisson, "The theoretical analysis of data compression systems," in *Proc. IEEE*, vol. 56, Feb. 1968, pp. 176–186.
[20] ——, "Information rates for data compression," *IEEE WESCON Tech. Papers*, Session B, Aug. 1968.
[21] D. Slepian, "On delta modulation," *Bell. Syst. Tech. J.*, vol. 51, pp. 2101–2137, Dec. 1972.
[22] J. B. Thomas, *An Introduction to Statistical Communication Theory*. New York: Wiley, 1969.
[23] M. D. Paez and T. H. Glisson, "Minimum mean-squared-error quantization in speech PCM and DPCM systems," *IEEE Trans. Commun.*, vol. COM-20, pp. 225–230, Ap. 1972.
[24] N. N. Lebedev, *Special Functions and Their Applications*. New York: Dover, 1972.
[25] R. M. Gray and Y. Linde, "Vector quantizers and predictive quantizers for Gauss–Markov sources," *IEEE Trans. Commun.*, vol. COM-30, pp. 381–389, Feb. 1982.
[26] D. G. Messerschmitt, "Quantizing for maximum output entropy," *IEEE Trans. Inform. Theory*, vol. IT-17, p. 612, Sept. 1971.
[27] R. G. Gallager, *Information Theory and Reliable Communication*. New York: Wiley, 1968.
[28] T. Berger, *Rate-Distortion Theory*. Englewood Cliffs, NJ: Prentice-Hall, 1971.
[29] H. Gish and J. N. Pierce, "Asymptotically efficient quantizing," *IEEE Trans. Inform. Theory*, vol. IT-14, pp. 676–683, Sept. 1968.
[30] D. L. Neuhoff and R. K. Gilbert, "Causal source codes," *IEEE Trans. Inform. Theory*, vol. IT-28, pp. 701–713, Sept. 1982.
[31] W. D. Hopkins, "Structural properties of rate distortion functions," Ph.D. thesis, Syst. Sci. Dept., Univ. of California, Los Angeles, 1972.
[32] R. M. Gray, "Information rates of autoregressive processes," *IEEE Trans. Inform. Theory*, vol. IT-16, pp. 412–421, July 1970.
[33] J. B. O'Neal, Jr., "Differential pulse-code modulation (PCM) with entropy coding," *IEEE Trans. Inform. Theory*, vol. IT-22, pp. 169–174, Mar. 1976.
[34] M. J. Carter and D. L. Neuhoff, "Bounds to the rate-distortion function for regenerative composite sources," in *Proc. 20th Allerton Conf. Commun., Control and Comput.*, Monticello, IL, Oct. 1982, pp. 680–681.
[35] R. E. Blahut, "Computation of channel capacity and rate-distortion functions," *IEEE Trans. Inform. Theory*, vol. IT-18, pp. 460–473, July 1973.
[36] J. W. Modestino, "Nonparametric and adaptive detection of dependent data," Ph.D. thesis, Electr. Eng. Dept., *Princeton Univ., Princeton, NJ, Apr.* 1969.
[37] E. Abaya and G. L. Wise, "Some notes on optimal quantization," in *Proc. IEEE Int. Conf. Commun.*, Denver, CO, June 1981, pp. 30.7–30.7.5.
[38] J. D. Gibson and T. R. Fischer, "Alphabet-constrained data compression," *IEEE Trans. Inform. Theory*, vol. IT-28, pp. 443–456, May 1982.